

Detonation structural response to multi-dimensional confinement

Jackson Crane^{1,*,#}, Jonathan T. Lipkowicz², Xian Shi¹,
Irenaeus Wlokas², Andreas M. Kempf², Hai Wang¹

¹ Department of Mechanical Engineering, Stanford University, Stanford, CA, USA

² Department of Fluid Dynamics, University of Duisburg–Essen, Duisburg, Germany

1 Introduction

Developing a better description of realistic multi-dimensional detonations hinges on understanding the structural features of detonations. Multi-dimensional detonations exhibit a characteristic cellular structure which reflects the propagation characteristics of detonations [1]. Detonation cells appear to correlate with detonation limits and remain one of the most measured and observed features of detonations [2, 3].

It is well-known that detonation confinement has a strong influence on its propagation characteristics. Indeed, if a geometry is substantially smaller than the characteristic cell size, detonations fail [4]. But confinement, or lack thereof, can also influence the cellular structure itself: partially unconfined detonations exhibit a cellular structure qualitatively different from those propagating in channels or tubes [5]. Detonations of practical interest (i.e., those in engines, accident scenarios, etc.) propagate in a wide variety of geometries, including unconfined spaces, and more often tubes and channels of various types. Therefore, understanding how detonation structure responds to various confinements is of both fundamental and practical significance.

This study aims to better understand and quantify detonation structural response to confinement by performing side-by-side 3D detonation simulations with two different geometries commonly used in experiments: square channels and round tubes. We will also contrast the 3D results to those from 2D simulations, which are often used to study detonation because they are less computationally expensive and easier to analyze than 3D simulations, and experimental results in tubes. This work presents, to our knowledge, the first ever well-resolved 3D detonation simulations in a tube geometry, and directly builds upon other past 3D simulation studies (mostly in rectangular channels, e.g. [6]). We solve the compressible Navier-Stokes equations with detailed chemistry (shown to be important by Taylor [7]) with isothermal and no-slip boundary conditions to provide the highest fidelity simulations possible. The mixture simulated is stoichiometric hydrogen-oxygen at 300 K and 15 kPa, with 3000 PPMv ozone doping. This mixture is chosen because it has been previously studied [8] and provides a relatively stable cellular structure that provides a basis to examine.

2 Numerical solver and setup

The simulations are performed with the in-house code *PsiPhi* [9, 10] that solves the fully compressible set of conservation equations for mass, momentum, total internal energy, and partial densities to simulate

* Correspondence to: jackson.crane@queensu.ca

Current address: Department of Chemical Engineering, Queen’s University, Kingston, Ontario, Canada

detonation wave propagation. The equations are discretized on an equidistant Cartesian grid utilizing the Finite Volume Method. An approximate Riemann solver computes convective fluxes at cell interfaces with the aid of a monotonicity preserving reconstruction scheme featuring a theoretical accuracy of 5th order, while a 2nd order central difference schemes is used for diffusive fluxes. A Strang Operator Splitting framework allows explicit time integration of convection and diffusion with a 3rd order accurate Runge-Kutta scheme, while the implicit solver CVODE advances the solution in time from reaction. Sub-filter dynamics are modeled with an eddy viscosity/diffusivity approach, and the filtered chemical source term is modeled with a tophat PDF that accounts for non-linear reaction rate constants. More details will be included in the final manuscript, and can also be found in [9, 10].

The reaction kinetics are modeled with the Foundational Fuel Chemistry Model Version 1.0 (FFCM-1) [11, 12] with the Princeton ozone sub-model [13]. Two 3D geometries are considered: a square channel 12 x 12 x 12 mm, and a tube 12 mm in diameter and 12 mm in length. The tube simulation is set up in a rectangular domain, where the effects of walls are modelled with the efficient immersed boundary technique. The boundary conditions used are no-slip and isothermal (300 K) for the walls, a Dirichlet boundary condition for the inlet, and a partially reflecting boundary condition for the outlet. This setup allows the numerical domain to be moved at CJ speed relative to the laboratory reference without wave reflection. Three numerical resolutions are simulated for each geometry: 40 μm , 20 μm , and 10 μm . The coarsest simulations are initialized with an inclined ZND detonation wave, while the finer simulations are initialized with a converged solution from the coarser resolutions. The macroscopic structural features were seen to converge at the 10 μm grid size. More detailed results of the convergence study shall be included in the full manuscript.

3 Results

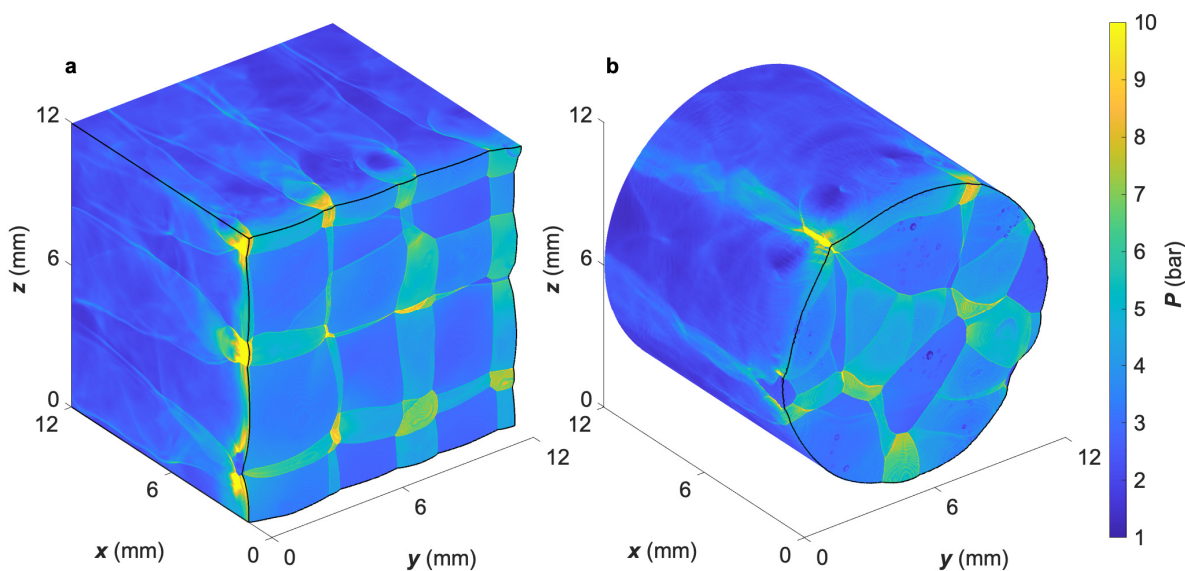


Figure 1: Isometric views of a single representative snapshot of the converged portion of the 3D channel simulations **a**) and 3D tube simulations **b**) at 20 μm grid resolution. Plotted is pressure pseudocolor, and the colorbar applies to both figures. Conditions in both simulations is stoichiometric hydrogen-oxygen with 3000 PPMv ozone additive at 15 kPa initial pressure.

Snapshots of a pressure pseudocolor are shown for both the 3D square channel (**a**) and tube (**b**) simula-

tions in Fig. 1. These snapshots are chosen in the well-converged portion of the simulations to exclude any memory effects from initial conditions. The two snapshots clearly show a substantial difference in the detonation structure between the two simulations. As other past researchers have observed [6, 14], the square channel exhibits a highly regular structure with ignition kernels occurring on a nearly perfectly spaced square grid. Although there are some deviations from the dominant structure (see upper right corner of Fig. 1a), the dominant structure is highly stable as evidenced that this structure is maintained throughout the entire simulation despite these deviations. The tube simulation, on the other hand, has no clearly discernible regular structure. Local shock waves of varying strength are observed throughout the detonation frontal structure, including reflections off the wall.

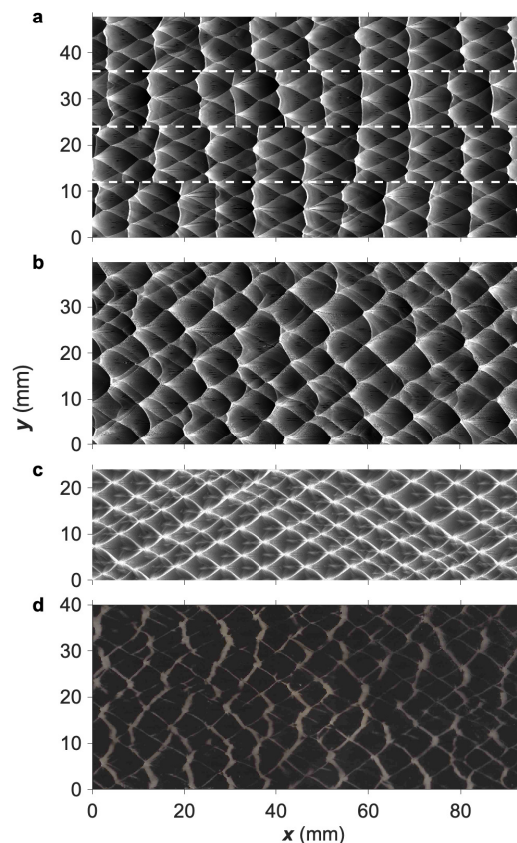


Figure 2: Numerical (**a**, **b**, **c**) and experimental (**d**) soot foils for identical mixture and conditions in different geometries. 3D square channel simulation **a**, with dashed white lines showing channel corners, 3D tube simulation **b**, 2D simulation **c**, and tube experiments **d**. All simulations at $10\ \mu\text{m}$ grid resolution.

Numerical soot foils are also calculated and compared for these simulations. The soot foils from 3D simulations are calculated by considering the pressure data near the shock front for computational simplicity, and so are an approximation of the full numerical soot foil. Nonetheless, they exhibit characteristic cellular features expected, and are useful to analyze and compare with 2D numerical soot foils and experimental soot foils. Figure 2 shows the soot foils for the 3D square channel (**a**) and tube (**b**) simulations as well as 2D simulations (**c**) and experiments (**d**), all with the same mixture and conditions (and in the case of the 3D and 2D simulations, at the same grid resolution of $10\ \mu\text{m}$). The experimental soot foil was obtained from a detonation tube experiment with tube inner diameter 32 mm [8]. Clearly seen from Fig. 2 is the differing structure among the various geometries. The square channel produces detonation cells which appear somewhat narrower and substantially longer as compared to those from the tube geometry. Meanwhile, the 2D simulation produces cells more characteristic of the tube simula-

tion, and the experimental soot foil and the 3D tube simulation also appear qualitatively similar. Notably missing from the 2D simulation is the white banding which appears transverse to the dominant cellular structure and shows out of plane transverse waves that collide with the wall. The square channel shows highly regular banding, while the 3D tube simulation and tube experiment show similarly more random banding.

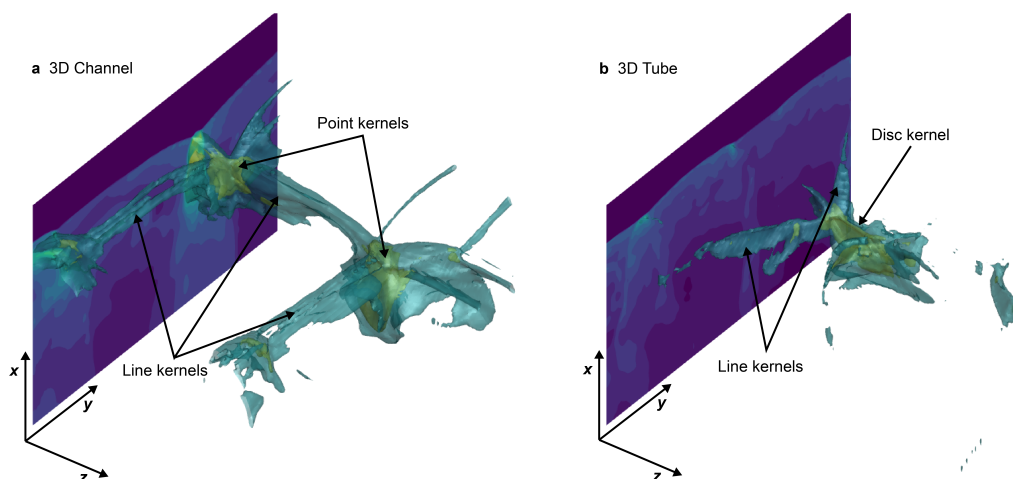


Figure 3: 6 bar (green) and 10 bar (yellow) isosurfaces from a single snapshot in time of the $40\ \mu\text{m}$ grid resolution simulation for the 3D channel **a** and 3D tube **b** simulations. Snapshots were selected to highlight kernel formation structure in each geometry.

To better understand the nature of the detonation structures, and resolve the differences between the 3D square channel and tube simulations, we analyze the detonation kernels. Detonation kernels (pockets of post-shock unburnt gas which experience rapid ignition after transverse wave collapse) are key to understanding cellular structure [15]. Figure 3 shows isosurfaces (6 bar and 10 bar) from sub-domains ($4 \times 4 \times 4\ \text{mm}$) of the square channel and tube simulations, with timesteps chosen to highlight the detonation kernels shortly after transverse wave collapse. Apparent in Fig. 3 are the different appearances of the kernels between the two simulations. The square channel exhibits what we shall call ‘line’ and ‘point’ kernels, where the line kernels result from two transverse waves collapsing, and the point kernels from four waves collapsing. As expected, the point kernels have a more extreme thermodynamic state after collapse than the line kernels. Meanwhile, the tube simulations exhibit similar line kernels, but instead of point kernels, they show more ‘disc’-like structures, which are resultant from 3 or 4 waves collapsing, sometimes not simultaneously.

We analyze the velocity characteristics of expanding shock waves originating from these various types of kernels, similarly to past work in 1D and 2D [15]. Shown in Fig. 4a is the velocity decay after ignition for 4 kernels of each type (i.e. Point and Line from square channels (3D C) and Disc and Line from tubes (3D T), as well as the velocity from 2D). The point and disc kernels have much higher velocities as compared to the line kernels, and the point kernel is somewhat faster than the disc kernels. Interestingly, the 2D kernels fall somewhat in between the point and line kernels. If the average velocity for an entire cell cycle is the CJ velocity (which will be approximately true on average, but not necessarily true for all cells), we can predict the cell size for a given velocity function. This calculation is shown in Fig. 4b, which shows the difference between the radial position of the blast (integrated wave velocity) and the radial position of a blast propagating at the CJ speed. The zero-crossing represents the duration of a cell. From this, we can derive a cell length, which is shown in Fig. 4c. As expected, point kernels yield the longest cells. These kernel dynamics can then be used to understand the differences in structures between the different geometries: the presence of these very strong point kernels lead to highly elongated

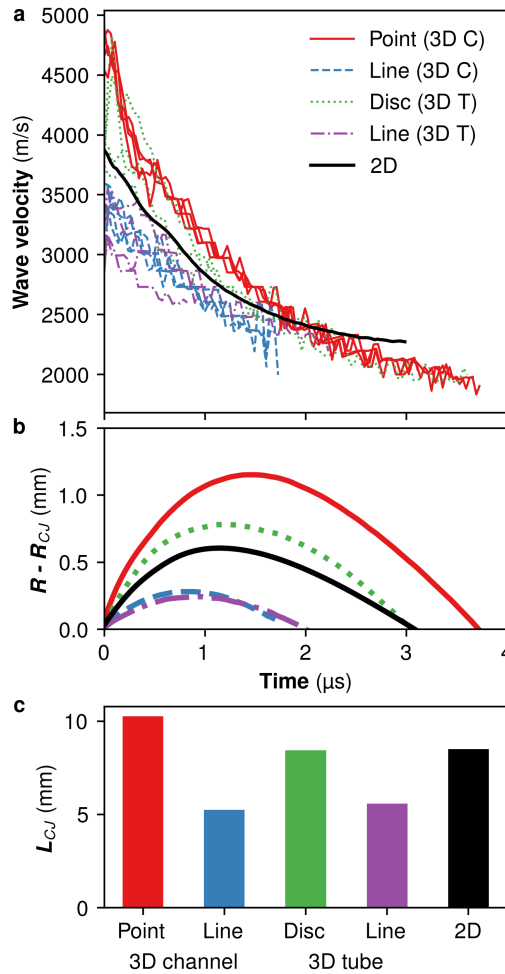


Figure 4: **a** Wave velocity after kernel ignition for point and line kernels in the 3D channel simulation, disc and line kernels in the 3D tube simulation (4 instances each), and 2D kernels. **b** The difference between the averaged, integrated blast radii and the radii of a blast traveling at the CJ velocity for each kernel type. **c** The predicted cell length for each kernel type if the blast has an average velocity of the CJ velocity. All analysis is performed on 10 μm simulations.

detonation cells, while the disc-like kernels from the tube lead to somewhat wider cells. More analysis and discussion will be included in the final manuscript and presentation.

4 Conclusions

From detailed 3D simulations of both square channel and tube geometries, we observe that the detonation structures are substantially different among the two geometries. Specifically, square channels yield highly regular grid-spaced kernels, while the tube exhibits a more chaotic structure similar to that measured from a tube experiment. Two kinds of kernels are observed in 3D detonations: a point (or disc) kernel which is from 3 or more blasts intersecting, and a line kernel, which is from two blasts intersecting. Interestingly, the 2D simulation kernels exhibit an average between the two main kernel types observed in 3D simulations.

References

- [1] J. H. Lee, *The detonation phenomenon*. Cambridge University Press, 2008.
- [2] M. I. Radulescu and J. H. Lee, “The failure mechanism of gaseous detonations: experiments in porous wall tubes,” *Combustion and Flame*, vol. 131, no. 1-2, pp. 29–46, 2002.
- [3] X. Shi, J. Crane, and H. Wang, “Detonation and its limit in small tubes with ozone sensitization,” *Proc. Combust. Inst.*, 2020.
- [4] F. Haloua, M. Brouillette, V. Lienhart, and G. Dupré, “Characteristics of unstable detonations near extinction limits,” *Combustion and Flame*, vol. 122, no. 4, pp. 422–438, 2000.
- [5] S. Murray and J. Lee, “On the transformation of planar detonation to cylindrical detonation,” *Combustion and Flame*, vol. 52, pp. 269–289, 1983.
- [6] C. Wang, C.-W. Shu, W. Han, and J. Ning, “High resolution WENO simulation of 3D detonation waves,” *Combustion and Flame*, vol. 160, no. 2, pp. 447–462, 2013.
- [7] B. D. Taylor, D. A. Kessler, V. N. Gamezo, and E. S. Oran, “Numerical simulations of hydrogen detonations with detailed chemical kinetics,” *Proc. Combust. Inst.*, vol. 34, no. 2, pp. 2009–2016, 2013.
- [8] J. Crane, X. Shi, A. V. Singh, Y. Tao, and H. Wang, “Isolating the effect of induction length on detonation structure: Hydrogen–oxygen detonation promoted by ozone,” *Combustion and Flame*, vol. 200, pp. 44–52, 2019.
- [9] M. Rieth, F. Proch, M. Rabaçal, B. M. Franchetti, F. C. Marincola, and A. M. Kempf, “Flamelet LES of a semi-industrial pulverized coal furnace,” *Combust. Flame*, vol. 173, pp. 39–56, 2016.
- [10] J. T. Lipkowicz, I. Wlokas, and A. M. Kempf, “Analysis of mild ignition in a shock tube using a highly resolved 3D-LES and high-order shock-capturing schemes,” *Shock Waves*, vol. 29, no. 4, pp. 511–521, 2019.
- [11] G. P. Smith, Y. Tao, and H. Wang, “Foundational fuel chemistry model version 1.0 (FFCM-1), <http://nanoenergy.stanford.edu/ffcm1>,” 2016.
- [12] Y. Tao, G. P. Smith, and H. Wang, “Critical kinetic uncertainties in modeling hydrogen/carbon monoxide, methane, methanol, formaldehyde, and ethylene combustion,” *Combustion and Flame*, vol. 195, pp. 18–29, 2018.
- [13] H. Zhao, X. Yang, and Y. Ju, “Kinetic studies of ozone assisted low temperature oxidation of dimethyl ether in a flow reactor using molecular-beam mass spectrometry,” *Combust. Flame*, vol. 173, pp. 187–194, 2016.
- [14] M. Hanana, M. Lefebvre, and P. Van Tiggelen, “On rectangular and diagonal three-dimensional structures of detonation waves,” *Gaseous and heterogeneous detonations: science to applications*, pp. 121–130, 1999.
- [15] J. Crane, X. Shi, J. T. Lipkowicz, A. M. Kempf, and H. Wang, “Geometric modeling and analysis of detonation cellular stability,” *Proc. Combust. Inst.*, 2020.